SHEAR STRENGTH OF SEDIMENT OFFSHORE SOUTHERN ALASKA

Senior Thesis
Submitted in partial fulfillment of the requirements for the
graduation with research distinction in Earth Sciences
in the undergraduate colleges of
The Ohio State University

By

Brandi L. Lenz
The Ohio State University
2017

Approved by

Dr. Derek Sawyer, Advisor

School of Earth Sciences

TABLE OF CONTENTS

ABSTRACT

The Surveyor Fan is the fourth largest submarine fan in the world and located in the Gulf of Alaska. The Surveyor Fan receives very high rates of sedimentation from the rapidly eroding St. Elias Mountains. Drilling during the Integrated Ocean Drilling Program (IODP) Expedition 341 in 2013 recovered 3240 m of sedimentary record from five sites within the Surveyor Fan. This project uses the shear strength data of the uppermost 100 meters to quantify the present-day slope stability of the fan. Shear strength is a measure of the sediment strength to withstand certain amounts of shear stress before it fails as a submarine landslide. Submarine landslides are capable of creating tsunamis. The Surveyor Fan is situated on an active seismic margin, therefore it is important to understand the risks and consequences of a submarine landslide because submarine landsliding events have happened in the recent past. Submarine landslides were generated by the magnitude-9.2 1964 Great Alaska earthquake at Valdez. The earthquake and submarine landslides created several tsunamis that ultimately killed 131 people as far away as California. This study shows a normal relationship of shear strength with depth, however the Surveyor Fan also has abnormally low values of shear strength for an active margin. This could be a major indicator that the Surveyor Fan is at high risk of slope failure.

ACKNOWLEDGEMENTS

I would like to first thank Dr. Derek Sawyer who gave me the opportunity to do research with him as an undergraduate. I would have had no idea how much I love studying submarine landslides if it were not for him. The knowledge and skills he has helped me develop throughout my two years at The Ohio State University will forever be a part of me as I continue to prepare for graduate school and future professional work. Without him I would not have been able to successfully write my thesis, let alone defend it. I also would like to thank Dr. Anne Carey for her amazing support throughout my undergraduate career and for teaching me the skills I need to write my thesis.

I need to thank my major advisor Dr. Karen Royce for meeting with me every semester making sure I was always on track. I also would like to thank Dr. Karen Royce and Dr. Anne Carey for their advice and guidance they provided me the year leading up to my admission into The Ohio State University. I would like to thank Dr. Michael Barton for allowing me to be a part of his research group. He taught me how to work with large data sets, which have become extremely useful tools. I need to also thank Dr. Terry Wilson. She is the best teacher that I have ever had. I couldn't think of a better person to teach structural geology or lead us during field camp. I have never learned so much information in such as short period of time, and in such a meaningful way.

I need to acknowledge the Integrated Ocean Drilling Program and their expedition 341 for collecting the data that I used for my thesis. I would also like to acknowledge Joshua DeVore whose paper with Dr. Derek Sawyer on elevated shear strength of sediments on active margins as evidence of seismic stregthenening helped inspire me to begin this research project. I also need to acknowledge the financial help I received along the way from the School of Earth

Sciences for the Willis E. “Bill” Rector Scholarship, the Edmund Spieker Memorial Scholarship, and the Earth Sciences Field Experience Travel Fund scholarship. I would like to thank Mrs. Janie Rector for not only the scholarship, but also for her encouragement and support.

Finaly I would like to thank The School of Earth Sciences, all my classmates, teachers, and teaching assistants. They have given me a home here. I would like to thank my friends, especially Taylor Hollis and Nick Rodgers. They have listened to all my complaints while writing this thesis, have helped me study and survive field camp, and just laughed with me. The memories we have made during our time here have been priceless. I would like to thank my family, especially my mother and father, Eva and Scott Bogdan. They taught me from a very young age that I could be anything that I wanted with hard work and perseverance. They knew my love for Earth Sciences and provided the support I needed to grow. Most importantly I would like to thank my husband, Gregory Lenz. None of this would have been possible without him. He put his life on pause just to help me pursue my dreams. I don’t think he will ever know how grateful I am for that. His love, support, and comfort were exactly what I needed to get where I am today. For that I will always be thankful.

List of Figures

LIST OF TABLES

INTRODUCTION

The focus of this study is on the undrained shear strength of sediments in the Surveyor Fan measured with the Geisa Automated Shear Vane (AVS) during IODP Expedition 341. Shear strength is represented as the torque required by the vane to shear the sediment. In other words, shear strength is the shear stress required for sediment failure. It is often defined by the Mohr-Coulomb failure criterion,

$$\tau_f = c' + (\sigma - u)\, tan\emptyset'$$

where τ_f is shear strength, c' is effective cohesion, σ is applied normal stress, u is pore water pressure, $(\sigma - u)$ represents the effective normal stress, and $\emptyset$ is the friction angle (Hampton et al., 1996). As the equation shows, there is a linear relationship between shear strength and effective normal stress. Therefore, we would expect there to be a linear relationship of shear strength with depth in the Surveyor Fan.

The purpose of this study is to quantify the slope stability of the Surveyor Fan. It is important to study slope stability because a major failure in the form of a submarine landslide poses significant risks to the coastal population. Submarine landslides have the potential to create tsunamis and have done so numerous times in the past. A great example of this happened during the 1964 Great Alaska earthquake at Valdez. The M-9.2 earthquake and the subsequent submarine landslides created tsunamis that killed over 131 people as far away as California. Not only do these kinds of geohazards pose human threats, but they also have great economic implications (Parsons et al., 2014).

Shear strength can be greatly affected by decreasing the effective stress. A common way effective stress can be reduced is by increasing the pore pressure. This will also result in a

decrease of shear strength and therefore a higher risk of slope failure (Hampton et al., 1996). High sedimentation rates of material with relatively low permeability can dramatically decrease the effective stress because it elevates the pore pressure of the sediments. (Hampton et al. 1996). Some studies have already looked at the correlation between submarine landslides and sedimentation rates. These studies showed that slope stability is decreased with an increase in sedimentation rate (Lee et al., 2004; Sawyer and DeVore, 2015; ten Brink et al., 2016).

Seismicity can also play a major role in slope stability. Several studies in the past decade have shown that slope stability is greater with an increase in earthquake frequency (Lee et al., 2004; Biscontin and Pestana, 2006; Sawyer and DeVore, 2015; ten Brink et al., 2016). Additonally, earthquakes are among the main triggers of slope failure by their induction of shear and normal stresses in sediment (Hampton and Lee, 1996). It is important to understand the seismic reponse of marine sediments for this study because the Surveyor Fan is located in an active seismic margin and earthquakes are a frequent event.

For this study, we looked at the relationship of shear strength with depth while analyzing the sediment characteristics of each site chosen to get a better understanding of the local slope stability. This will allow us to see what areas need to be explored further and will guide what direction future research in the Surveyor Fan should go to protect life and property of the coastal population.

GEOLOGIC SETTING

Geology

The study area for this research project is the Surveyor Fan which is the fourth largest submarine fan in the world and is located in the Gulf of Alaska off the continental margin of southern Alaska. The Surveyor Fan is situated on an active seismic margin due to its proximity towhere the Pacific plate collides with and subducts under the North American plate. The subduction occurs along the Aleutian Trench in the western part of the Gulf of Alaska and the flat-slab subduction has created the still-active Chugach-St. Elias Orogen (Carlson, 1989; Reece et al., 2011).

The Surveyor Fan is on the Pacific plate and covers over 300,000 km^2. It has been active since at least the Miocene and within the past 1.2 million years, glacial erosion from the St. Elias Mountain Range has provided huge amounts of sediment, even more so than the tectonic input (Gulick et al., 2015). The fan is fed by the Chirikof and Surveyor Channel System which are large deep water channels that are unassociated with any fluvial systems and thus unlike most channels in the world (Reece et al., 2011).

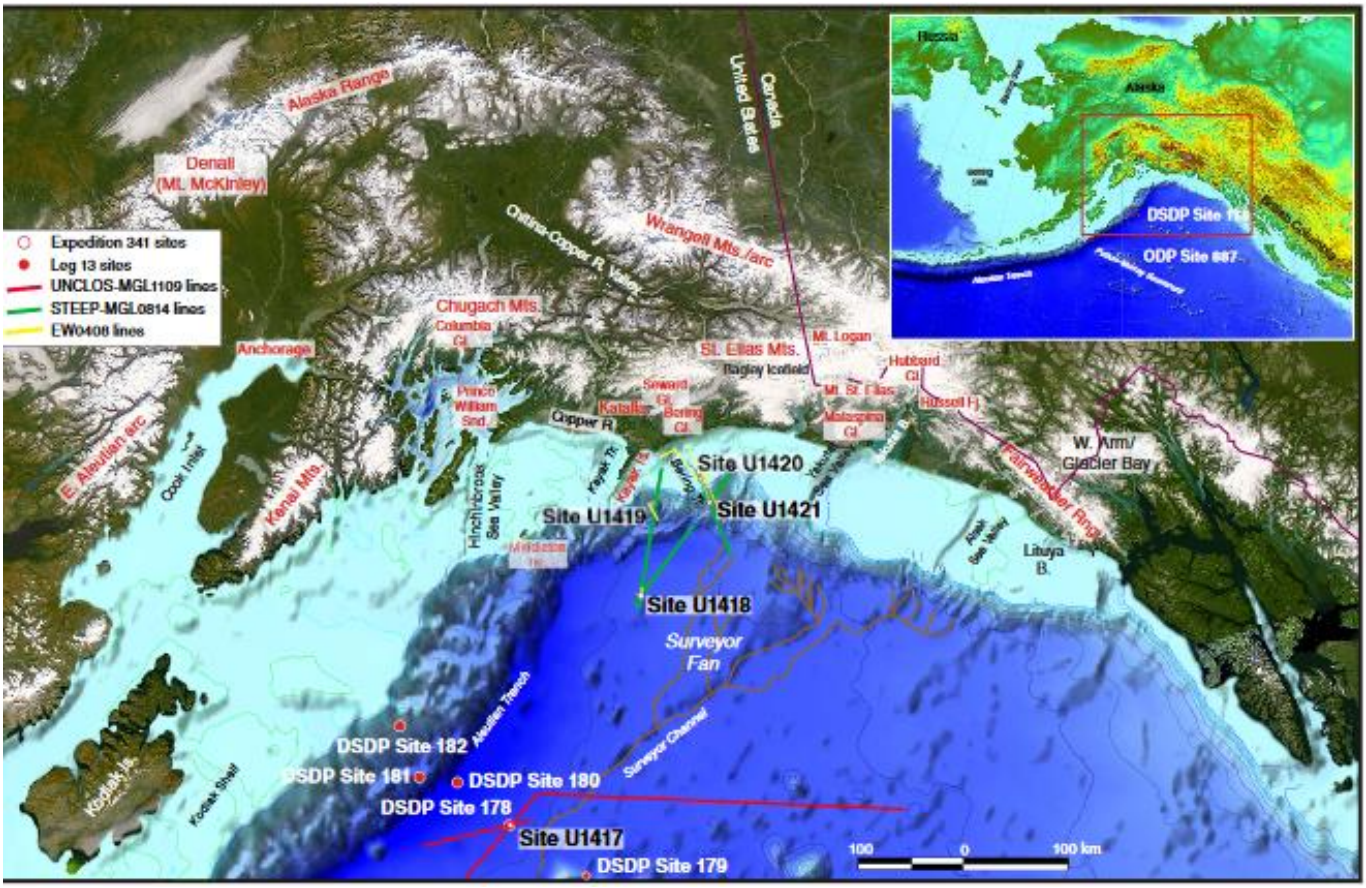

Figure 1: Map of IODP Expedition 341 showing all drill sites. From Expedition 341 Scientists (2013).

Past Tectonic Activity

The Gulf of Alaska is a high seismically active zone due to the ongoing collision of the Pacific and North American plates. The collision of these two plates has been responsible for numerous large destructive earthquakes and tsunamis in the past such as the magnitude-9.2 1964 Great Alaska Earthquake that originated from Prince William Sound. The earthquake and submarine landslides created several tsunamis that ultimately killed 131 people as far away as California (Parsons et al., 2014).

There have been other large earthquakes that have occurred in the Gulf of Alaska. Probably the most famous example is the 1987–88 Gulf of Alaska sequence. This sequence consisted of three large earthquakes registering as 6.9, 7.6, and 7.6 magnitudes respectively. These earthquakes were unusual because they occurred away from the Aleutian trench within the Pacific plate where there was no known seismic activity. Strike-slip faulting within the plate was responsible for producing these earthquakes proving just how complex and dangerous the Gulf of Alaska geology is to the coastal populations of the region (Hwang and Kanamon, 1992).

METHODS

During IODP Expedition 341, shear strength was measured with the Giesa Automated Vane Shear (AVS). This device is a four-bladed miniature vane that is commonly used for measuring shear strength of soft marine sediments. It is not useful for determining shear strength in coarser grained sediments. The IODP Expedition 341 scientists used the JOIDES Resolution research vessel to core sediment at five different sites. Once shipboard, they pushed the vane into the sediment of the cores until the top of the vane was level with the surface of the sediment. They then rotated the vane at a constant rate of 90°per minute. The torque required to shear the sediment is recorded and used to convert to undrained shear strength given in units of pascals. They repeated this measurement for every core section (about every four meters) until their plot curve showed a decrease (Expedition 341 Scientists, 2013).

SITE LOCATIONS

Only sites from IODP Expedition 341 containing mostly fine-grained mud in the top 100 meters with continuous sedimentation and lacking evidence of unconformities and submarine land sliding were used. Chosen were U1417, U1418, U1419, and U1421. Excluded was site U1420.

Site U1417 is at about 4200 m water depth and located in the distal Surveyor Fan. It is fed with sediment by overbank processes from the Surveyor Channel which is about 60 km away. This site was chosen by IODP Expedition 341 scientists to provide a sedimentary record of Neogene glacial and tectonic processes of the St. Elias orogeny that is still ongoing today. The top 100 meters of interest consist of only one lithological unit (Unit I) that is divided into two different subunits (Subunit IA and Subunit IB). Both subunits are made of mostly dark gray mud with locally occurring lonestones and intervals of diatom ooze and minor interbeds of volcanic ash, however Subunit IB has more frequent intervals of diatom ooze. Based on shipboard smearslides, the mud is made up of about 90% clay sized particles and 10% silt sized particles. Sedimentation rates are about 0.13 mm/yr (Expedition 341 Scientist, 2013).

Site U1418 is at 3703 m water depth and located in the proximal Surveyor Fan between the Aleutian Trench and the Bering Channel. It is fed by sediment settling and sediment gravity flows from adjacent channels. This site was chosen by IODP Expedition 341 scientists to provide a sedimentary record of the late Pleistocene to get a better understanding of the dynamics and timing of glacial events. The top 100 meters of interest consist of only one lithological unit (Unit I). It is made of mostly dark gray mud with interbedded silt and mud alternates. Based on shipboard smearslides, the mud is made up of about 75% clay sized particles and 25% silt sized particles. Sedimentation rates are about 0.88 mm/yr, which is almost

a six-fold increase from site U1417. This is mostly due to being closer to the orogeny that is responsible for most of the deposition within the fan (Expedition 341 Scientists, 2013; Gulick et al., 2015).

Site U1419 is at 721 m water depth and is located on the Khitrov Bank which is on the continental slope above the Khitrov Ridge. It is influenced by the Alaska Coastal Current. This site was chosen by IODP Expedition 341 scientists to provide a sedimentary record of the late Pleistocene to get a better understanding of glacial events and sea-surface temperatures. The top 100 meters of interest consists of only one lithological unit (Unit I). It is made of mostly olive gray diatom ooze with intervals of ooze and diatom-rich mud. Based on shipboard smearslides, the mud is made up of about 70–80% clay sized particles and 20–30% silt sized particles. This site experiences the highest sedimentation rate , about 3 mm/yr due, to its location on the slope.

Site U1421 is at about 721 m water depth. It is located downslope the Bering Trough on the continental slope. The site was chosen by IODP Expedition 341 scientists to understand the actively deforming orogenic strctures and the impact of the sedimentation rates changing in the Neogene. The top 100 meters of interest consist of only two lithological units (Unit I and Unit II). They are made of mostly dark greenish gray diatom rich mud, however Unit II includes intervals of diamict. Sedimentation rates along this part of the slope are about 2.3 mm/yr (Expedition 341 Scientists, 2013).

For this research project, U1420 was not chosen because it is not made up of mostly fine-grained marine sediment. The top 100 meters of interest only consist of two lithological units (Unit I and Unit II). They were both very clast rich and also penetrate through an angular uncomformity which makes it not an ideal site to analyze shear strength. Sedimentation rates

here along the shelf were at about 1.3 mm/yr (Expedition 341 Scientists, 2013; Sawyer and DeVore, 2015).

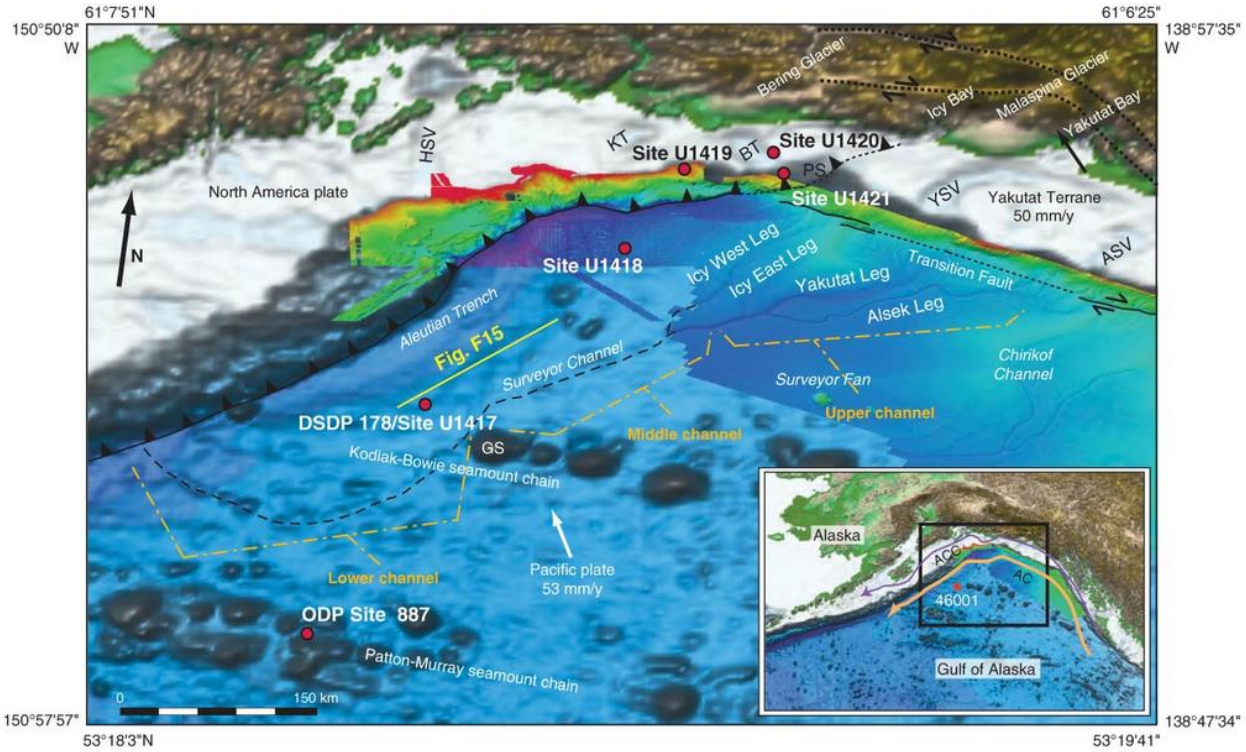

Figure 2: Map of IODP Expedition 341 showing detailed location map of all drill sites. From Expedition 341 Scientists (2013).

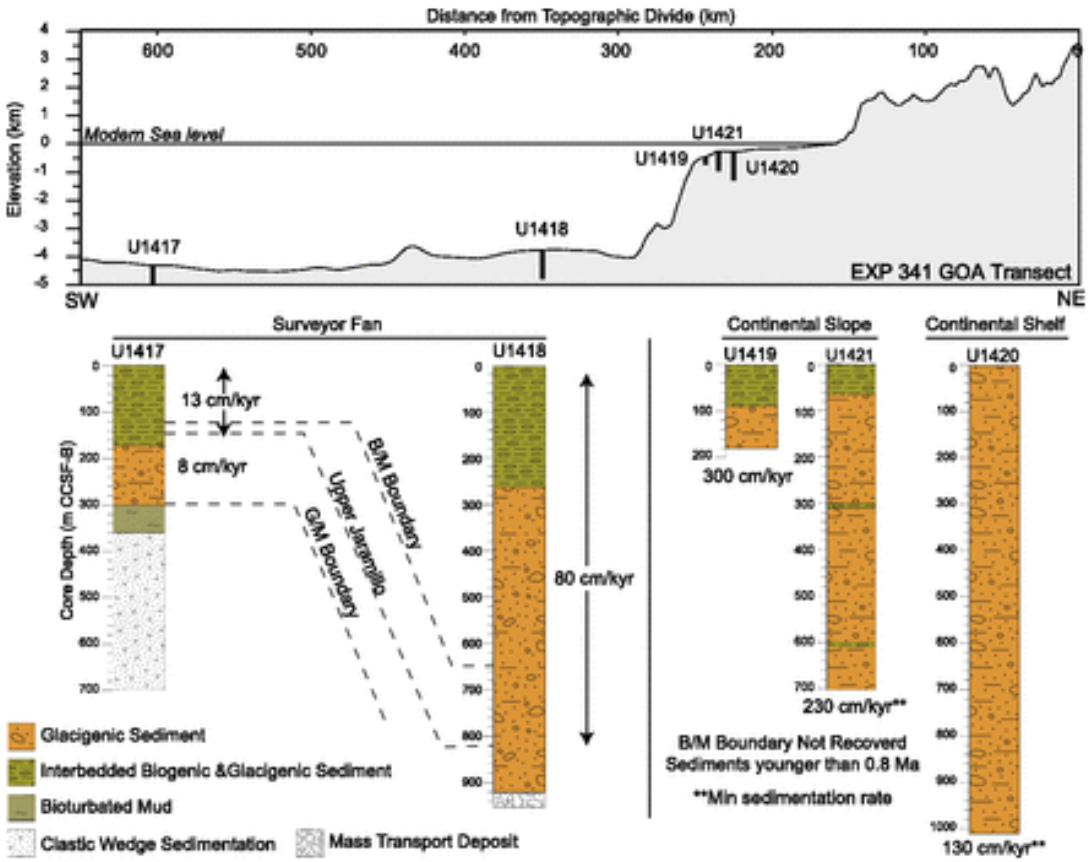

Figure 3: Cross-sectional topography profile showing location of all five sites; and their principal lithologies with sedimentation rates in centimeters per thousand years. From (Gulick et al., 2015).

RESULTS

Shear Strength vs Depth

Shear strength was compared with depth in several plots. One comparision used the top 100 meters of shear strength data with depth (Figure 4), and another used only the top 20 meters (Figure 5). Both plots showed the expected relationship of shear strength increasing with depth and displayed average shear strength values that are expected of fine grained silicilastic sediments with high sedimentation rates (Gulick et al., 2015; Bartetzko and Kopf, 2007; Hamilton, 1971). IODP Expedition 341 site U1417 showed the highest average shear strength in the uppermost 20 meters at 14.152 kPa. Site U1418 had the lowest average shear strength in the uppermost 20 meters at 8.578 kPa. The average shear strength in the uppermost 20 meters for all of the sites compared was 11.315 kPa.

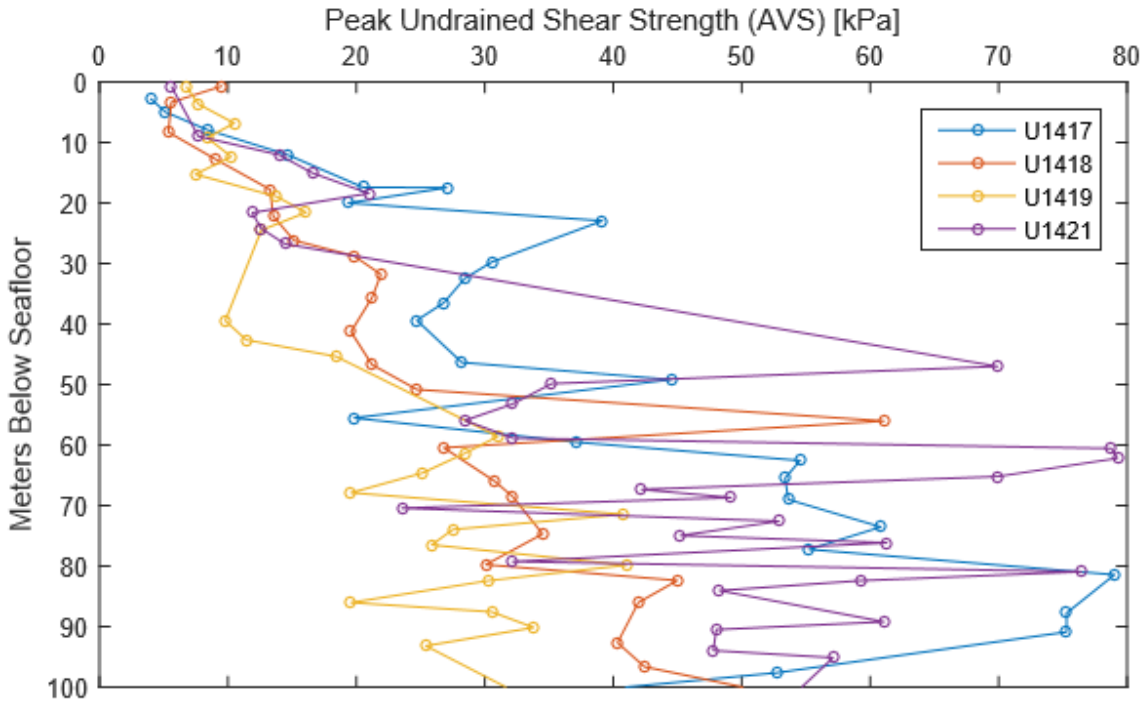

Figure 4: Plot showing peak undrained shear strength measured with the Geisa Automated Shear Vane (AVS) in kPa versus 100 meters depth below the seafloor for four different sites from IODP Expedition 341.

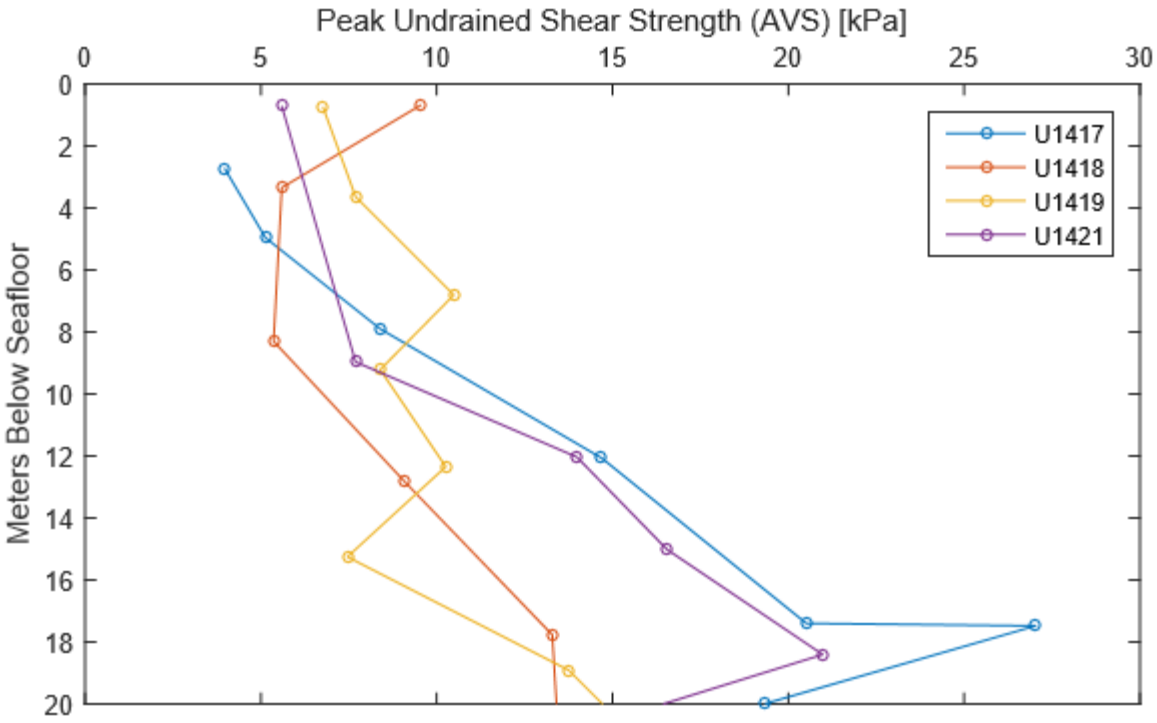

Figure 5: Plot showing peak undrained shear strength measured with the Geisa Automated Shear Vane (AVS) in kPa versus the top 20 meters depth below the seafloor for four different sites from IODP Expedition 341.

Discussion

Surveyor Fan Shows Passive Margin Behavior

The Surveyor Fan showed a normal relationship of shear strength increasing with depth and displayed average shear strength values that are expected of fine grained silicilastic sediments (Bartetzko and Kopf, 2007; Hamilton, 1971). Because of the Surveyor Fan's location on an active margin, processes of seismic strengthening should have caused the shear strength to be higher than what was recorded (Sawyer and DeVore, 2015).

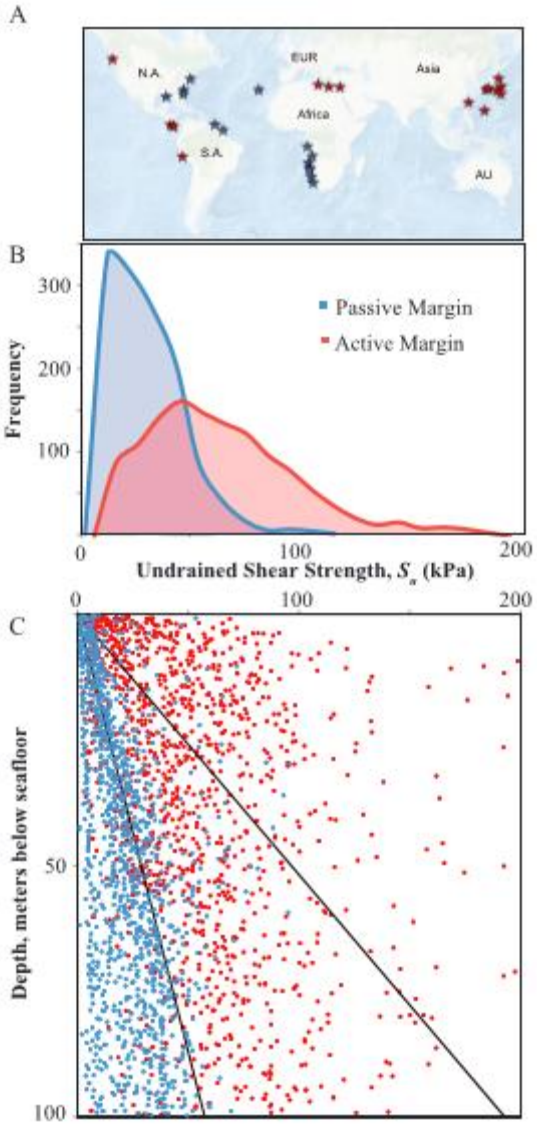

Figure 6: A) Sites used in Sawyer & DeVore's study. Active margins are from Japan, Costa Rica, Peru, Cascadia, and the Mediterranean. Passive margins are from New Jersey, Gulf of Mexico, Amazon Fan, Madeira, and West Africa. B) Graph from Sawyer & DeVore's study showing the normal distribution of shear strength. C) Undrained shear strength versus depth of all sites from Sawyer & DeVore's study. Blue points represent passive margins and red points represent active margins. The trend lines represent the arithmetic means of each margin type. From Sawyer and DeVore (2015).

According to Sawyer and DeVore, active margins have higher undrained shear strength than passive margins and they have demonstrated this with 67 sites globally where AVS shear strength data were collected. A plot of the Expedition 341 sites with 6 other sites (3 passive and 3 active sites) that were also measured with AVS, the Surveyor Fan clearly acts as a passive margin not an active one (Figure 7).

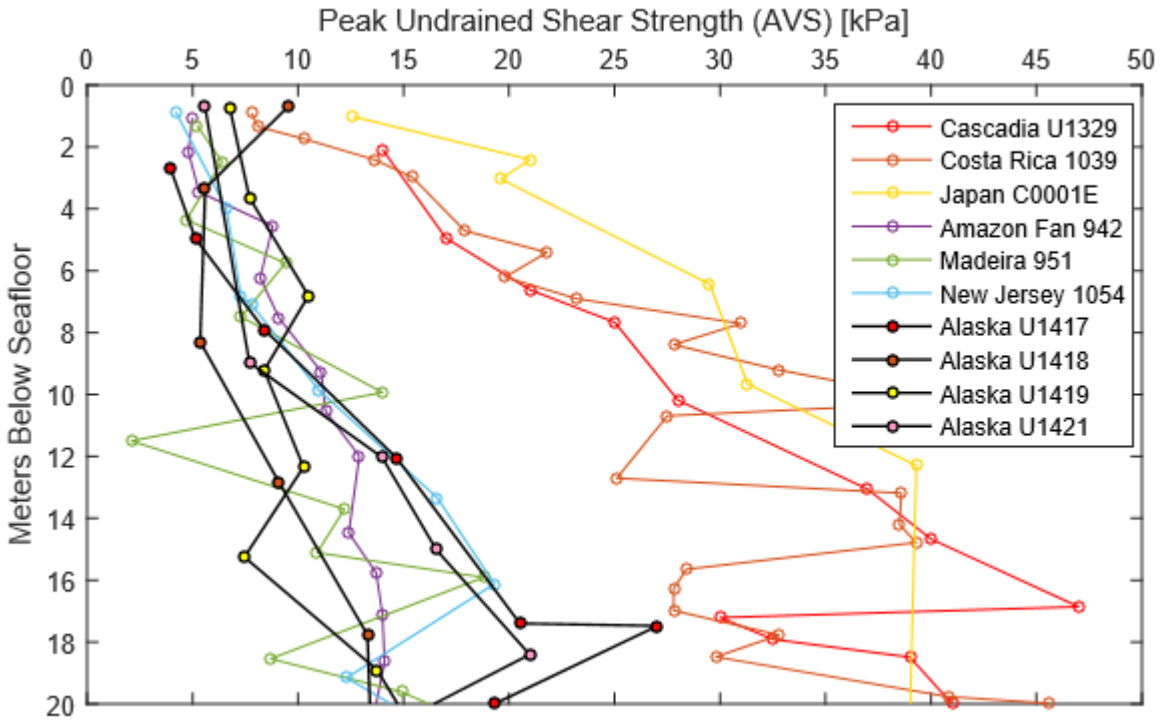

Figure 7: Peak undrained shear strength measured with Automated Shear Vane (AVS) in kPa versus the top 20 meters depth below the seafloor to compare the Surveyor Fan with other margins in the world. Active margins included are Cascadia, Costa Rica, and Japan. Passive margins included at Amazon Fan, Madeira, and New Jersey.

The Surveyor Fan shows behaviors of shear strength with depth similar to behavior seen in passive margins (Figure 7). Another factor that needs to be considered in evaluation of shear strength is sedimentation rate. The Surveyor Fan is the fourth largest submarine fan in the world

and receives an anomalously high rate of sedimentation (Gulick et al., 2015). The shear strengths observed in the Surveyor Fan suggest that it may be over-pressured due to rapid deposition (Gibson, 1958; Bredehoeft and Hanshaw, 1968; Fowler and Yang, 1998; Dugan and Flemings, 2000; Wolinsky and Pratson, 2007).

Implications for Submarine Landslides & Tsunami Hazards

According to previous studies, a correlation between submarine landslides and earthquake frequencies has been observed supporting the idea of seismic strengthening. It is shown that slope stability is greater with an increase of earthquake activity(Lee et al., 2004; Bisontin and Pestana, 2006; Sawyer and DeVore, 2015; ten Brink et al., 2016). In studies of the correlation between submarine landslides and sedimentation rates, some studies showed that slope stability is decreased with an increase in sedimentation rate (Lee et al., 2004; Sawyer and DeVore, 2015; ten Brink et al., 2016). Elevated pore pressures caused by high sedimentation rates are considered a major preconditioning factor in submarine landslide events, however earthquakes are thought to be the main triggering mechanism (Keefer, 1984; Biscontin and Pestana, 2006; Harbitz et al., 2014).

The Surveyor Fan seems to be a recipe for disaster, since it experiences both a high rate of sedimentation and a high frequency of earthquake activity. These are dangerous conditions for the residents along the coast of Alaska and the western United States, since submarine landslides can cause tsunamis and have caused them in the recent past. Submarine landslide induced tsunamis can be especially dangerous because they could enhance tsunami events that were originally caused by the earthquake rupture itself, can also occur locally giving residents little to no time to react, and are very difficult to monitor and predict (Harbitz et al., 2014).

CONCLUSIONS

The Surveyor Fan shows a normal relationship of shear strength with depth for siliciclastic sediments. It also has abnormally low values of shear strength for an active margin that may be explained by elevated pore pressures caused by anomalously high sedimentitation rates. The Surveyor Fan may be at high risk for slope failure in the future of a large magnitude and duration earthquake event.

RECOMMENDATIONS FOR FUTURE WORK

Possible future work could be to create a Factor of Safety map using Stigall and Dugan's methods and importing the data into ArcGIS to determine how unstable the slopes of the Surveyor Fan are currently and what areas may be at high risk. To do this, measurements and calculations for sediment cohesion for effective stress, total vertical stress, hydrostatic pore pressure, seafloor slope angles, angle of internal friction for effective stress, and overpressure are required (Stigall and Dugan, 2010).

REFERENCES CITED

Bartetzko, A., and Kopf, A. J., 2007, The relationship of undrained shear strength and porosity with depth in shallow (< 50 m) marine sediments: *Sedimentary Geology, 196*(1), 235-249.

Biscontin, G., and Pestana, J. M., 2006, Factors affecting seismic response of submarine slopes: *Natural Hazards and Earth System Science, 6*(1), 97-107.

Bredehoeft, J.D., and Hanshaw, B. B., 1968, On the maintenance of anomalous fluid pressures: I. Thick sedimentary sequences: *Geological Society of America Bulletin, 79*(9), 1097-1106.

Carlson, P. R., 1989, Seismic reflection characteristics of glacial and glacimarine sediment in the Gulf of Alaska and adjacent fjords: *Marine Geology, 85*(2-4), 391-416.

Dugan, B., and Flemings, P. B., 2000, Overpressure and fluid flow in the New Jersey continental slope: implications for slope failure and cold seeps: *Science, 289*(5477), 288-291.

Expedition 341 Scientists, 2013, Southern Alaska Margin: Integrated Ocean Drilling Program Management International, Inc.

Fowler, A. C., and Yang, X. S., 1998, Fast and slow compaction in sedimentary basins: *SIAM Journal on Applied Mathematics, 59*(1), 365-385.

Gibson, R. E., 1958, The progress of consolidation in a clay layer increasing in thickness with time: *Geotechnique, 8*(4), 171-182.

Gulick, S. P., Jaeger, J. M., Mix, A. C., Asahi, H., Bahlburg, H., Belanger, C. L., Berbelg, G.B.B., Childress, L., Cowan, E., Drab, L., Forwick, M., Fukumura, A., Ge, S., Gupta, S., Kioka, A., Konno, S., LeVay, L.J., März, C., Matsuzaki, K.M., McClymont, E.L., Moy, C., Müller, J., Nakamura, A., Ojima, T., Ribeiro, F.R., Ridgway, K.D., Romero, O.E., Slagle, A.L., Stoner, J.S., St-Onge, G., Suto, I., Walczak, M.D., Worthington, L.L., Bailey, I., Enkelmann, E., Reece, R., and Swartz, J.M, 2015, Mid-Pleistocene climate transition drives net mass loss from rapidly uplifting St. Elias Mountains, Alaska: *Proceedings of the National Academy of Sciences, 112*(49), 15042-15047.

Hamilton, E. L., 1971, Elastic properties of marine sediments: *Journal of Geophysical Research, 76*(2), 579-604.

Hampton, M. A., Lee, H. J., and Locat, J, 1996, Submarine landslides: *Reviews Of Geophysics, 34*(1), 33-59.

Harbitz, C. B., Løvholt, F., and Bungum, H, 2014, Submarine landslide tsunamis: how extreme and how likely?: *Natural Hazards, 72*(3), 1341-1374.

Hwang, L. J., and Kanamori, H., 1992, Rupture processes of the 1987–1988 Gulf of Alaska earthquake sequence: *Journal of Geophysical Research: Solid Earth, 97*(B13), 19881-19908.

Keefer, D. K., 1984, Landslides caused by earthquakes: *Geological Society of America Bulletin, 95*(4), 406-421.

Lee, H. J., Orzech, K., Locat, J., Konrad, J. M., and Boulanger, E, 2004, Seismic strengthening, a conditioning factor influencing submarine landslide development: *57th Canadian Geotechnical Conference*, Vol. 57, p. 7.

Parsons, T., Geist, E. L., Ryan, H. F., Lee, H. J., Haeussler, P. J., Lynett, P., Hart, P.E., Sliter, R., and Roland, E, 2014, Source and progression of a submarine landslide and tsunami; the 1964 great Alaska earthquake at Valdez: *Journal Of Geophysical Research: Solid Earth*, *119*(11), 8502-8516.

Reece, R. S., Gulick, S. P., Horton, B. K., Christeson, G. L., and Worthington, L. L., 2011, Tectonic and climatic influence on the evolution of the Surveyor Fan and Channel system, Gulf of Alaska: *Geosphere*, *7*(4), 830-844.

Sawyer, D. E., and DeVore, J. R, 2015, Elevated shear strength of sediments on active margins: Evidence for seismic strengthening: *Geophysical Research Letters*, *42*(23).

Stigall, J., and Dugan, B, 2010, Overpressure and earthquake initiated slope failure in the Ursa region, northern Gulf of Mexico: *Journal of Geophysical Research: Solid Earth*, *115*(B4).

ten Brink, U. S., Andrews, B. D., and Miller, N. C., 2016, Seismicity and sedimentation rate effects on submarine slope stability: *Geology*, *44*(7), 563-566.

Wolinsky, M. A., and Pratson, L. F., 2007, Overpressure and slope stability in prograding clinoforms: Implications for marine morphodynamics: *Journal of Geophysical Research: Earth Surface*, *112*(F4).

APPENDIX

Table 1: Data from Site U1417

Exp	Site	Hole	Core	Type	Sect	A/W	Offset (cm)	Depth CSF-A (m)	Depth CSF-B (m)	Vane shear strength (N/m²)	Max torque angle (deg)	Penetration direction	Vane rotation rate (deg/s)	Timestamp (UTC)	Instrument	Text ID	Test No.
341	U1417	A	1	H	2	W	125	2.75	2.71	3.963	10	X	1	6/6/2013 6:10	AVS	SHLF4631931	4.5E+07
341	U1417	A	1	H	4	W	53	5.03	4.957	5.128	14	X	1	6/6/2013 2:27	AVS	SHLF4631991	4.5E+07
341	U1417	A	2	H	2	W	112	8.02	7.897	8.391	15	X	1	6/6/2013 5:28	AVS	SHLF4632461	4.5E+07
341	U1417	A	2	H	5	W	99	12.39	12.061	14.685	24	X	1	6/6/2013 5:40	AVS	SHLF4632551	4.5E+07
341	U1417	A	3	H	2	W	107	17.47	17.399	20.512	17	X	1	6/6/2013 17:18	AVS	SHLF4633151	4.5E+07
341	U1417	A	3	H	2	W	115	17.55	17.477	27.038	24	X	1	6/6/2013 7:52	AVS	SHLF4633151	4.5E+07
341	U1417	A	3	H	4	W	73	20.13	19.986	19.346	17	X	1	6/6/2013 17:31	AVS	SHLF4633211	4.5E+07
341	U1417	A	3	H	6	W	76	23.16	22.932	39.159	24	X	1	6/6/2013 18:09	AVS	SHLF4633271	4.5E+07
341	U1417	A	4	H	4	W	122	30.13	29.747	30.535	19	X	1	6/6/2013 8:13	AVS	SHLF4633761	4.5E+07
341	U1417	A	4	H	6	W	120	33.03	32.453	28.437	23	X	1	6/6/2013 8:27	AVS	SHLF4633821	4.5E+07
341	U1417	A	5	H	2	W	108	36.48	36.48	26.805	25	X	1	6/6/2013 9:45	AVS	SHLF4634261	4.5E+07
341	U1417	A	5	H	4	W	98	39.38	39.38	24.708	17	X	1	6/6/2013 9:45	AVS	SHLF4634321	4.5E+07
341	U1417	A	7	H	2	W	2	46.42	46.337	28.204	26	X	1	6/6/2013 15:41	AVS	SHLF4635011	4.5E+07
341	U1417	A	7	H	4	W	2	49.42	49.173	44.52	12	X	1	6/6/2013 15:41	AVS	SHLF4635071	4.5E+07
341	U1417	A	8	H	1	W	112	55.52	55.515	19.813	12	X	1	6/6/2013 23:39	AVS	SHLF4635701	4.5E+07
341	U1417	A	9	H	2	W	110	59.5	59.5	37.061	14	X	1	6/6/2013 21:41	AVS	SHLF4636181	4.5E+07
341	U1417	A	9	H	4	W	115	62.55	62.55	54.543	22	X	1	6/6/2013 21:49	AVS	SHLF4636241	4.5E+07
341	U1417	A	9	H	6	W	104	65.44	65.44	53.378	11	X	1	6/6/2013 21:59	AVS	SHLF4636301	4.5E+07
341	U1417	A	10	H	2	W	115	69.05	68.987	53.611	12	X	1	6/7/2013 0:41	AVS	SHLF4636981	4.5E+07
341	U1417	A	10	H	5	W	130	73.7	73.528	60.836	17	X	1	6/7/2013 0:41	AVS	SHLF4637071	4.5E+07
341	U1417	A	11	H	1	W	132	77.22	77.22	55.242	16	X	1	6/7/2013 3:53	AVS	SHLF4637381	4.5E+07
341	U1417	A	11	H	4	W	102	81.42	81.42	79.018	12	X	1	6/7/2013 3:53	AVS	SHLF4637471	4.5E+07
341	U1417	A	12	H	2	W	91	87.81	87.741	75.288	12	X	1	6/7/2013 5:46	AVS	SHLF4638141	4.5E+07
341	U1417	A	12	H	4	W	114	91.04	90.878	75.288	14	X	1	6/7/2013 5:46	AVS	SHLF4638201	4.5E+07
341	U1417	A	13	H	2	W	123	97.63	97.63	52.678	15	X	1	6/7/2013 7:26	AVS	SHLF4638601	4.5E+07

Table 2: Data from Site U1418

Exp	Site	Hole	Core	Type	Sect	A/W	Offset (cm)	Depth CSF-A (m)	Depth CSF-B (m)	Vane shear strength (N/m²)	Max torque angle (deg)	Penetration direction	Vane rotation rate (deg/s)	Timestamp (UTC)	Instrument	Text ID	Test No.
341	U1418	A	1	H	1	W	68	0.68	0.67	9.557	15	X	1	6/24/2013 23:15	AVS	SHLF4701741	4.6E+07
341	U1418	A	1	H	3	W	39	3.39	3.341	5.594	12	X	1	6/24/2013 23:15	AVS	SHLF4701801	4.6E+07
341	U1418	A	2	H	3	W	50	8.3	8.3	5.361	12	X	1	6/25/2013 23:26	AVS	SHLF4702271	4.6E+07
341	U1418	A	2	H	6	W	53	12.83	12.83	9.091	12	X	1	6/25/2013 23:26	AVS	SHLF4702361	4.6E+07
341	U1418	A	3	H	3	W	53	17.83	17.768	13.286	12	X	1	6/25/2013 23:27	AVS	SHLF4702771	4.6E+07
341	U1418	A	3	H	6	W	48	22.28	22.14	13.519	17	X	1	6/25/2013 23:27	AVS	SHLF4702861	4.6E+07
341	U1418	A	4	H	2	W	95	26.25	26.18	15.151	12	X	1	6/26/2013 2:32	AVS	SHLF4703391	4.6E+07
341	U1418	A	4	H	4	W	57	28.87	28.725	19.813	12	X	1	6/26/2013 7:00	AVS	SHLF4703451	4.6E+07
341	U1418	A	4	H	6	W	73	32.03	31.795	21.91	17	X	1	6/26/2013 7:00	AVS	SHLF4703511	4.6E+07
341	U1418	A	5	H	2	W	90	35.7	35.66	21.211	14	X	1	6/25/2013 1:14	AVS	SHLF4704041	4.6E+07
341	U1418	A	5	H	6	W	60	41.4	41.266	19.58	16	X	1	6/25/2013 5:06	AVS	SHLF4704161	4.6E+07
341	U1418	A	6	H	3	W	107	46.87	46.694	21.211	22	X	1	6/25/2013 23:25	AVS	SHLF4704611	4.6E+07
341	U1418	A	6	H	6	W	88	51.18	50.817	24.708	26	X	1	6/25/2013 23:25	AVS	SHLF4704701	4.6E+07
341	U1418	A	7	H	3	W	88	56.18	56.027	61.07	17	X	1	6/25/2013 23:26	AVS	SHLF4705561	4.6E+07
341	U1418	A	7	H	6	W	97	60.77	60.436	26.805	17	X	1	6/25/2013 23:26	AVS	SHLF4705651	4.6E+07
341	U1418	A	8	H	3	W	120	66	65.978	30.768	17	X	1	6/25/2013 23:26	AVS	SHLF4705971	4.6E+07
341	U1418	A	8	H	5	W	76	68.56	68.525	32.166	14	X	1	6/25/2013 23:26	AVS	SHLF4706031	4.6E+07
341	U1418	A	9	H	3	W	45	74.75	74.679	34.497	26	X	1	6/25/2013 23:27	AVS	SHLF4706341	4.6E+07
341	U1418	A	9	H	6	W	113	79.93	79.753	30.069	21	X	1	6/25/2013 23:27	AVS	SHLF4706431	4.6E+07
341	U1418	A	10	H	2	W	55	82.37	82.37	44.986	15	X	1	6/25/2013 23:27	AVS	SHLF4707101	4.6E+07
341	U1418	A	10	H	5	W	55	85.99	85.99	41.956	15	X	1	6/25/2013 23:27	AVS	SHLF4707191	4.6E+07
341	U1418	A	11	H	2	W	92	92.72	92.641	40.325	21	X	1	6/25/2013 23:27	AVS	SHLF4707541	4.6E+07
341	U1418	A	11	H	5	W	54	96.84	96.627	42.422	26	X	1	6/25/2013 23:27	AVS	SHLF4707631	4.6E+07

Table 3: Data from Site U1419

Exp	Site	Hole	Core	Type	Sect	A/W	Offset (cm)	Depth CSF-A (m)	Depth CSF-B (m)	Vane shear strength (N/m²)	Max torque angle (deg)	Penetration direction	Vane rotation rate (deg/s)	Timestamp (UTC)	Instrument	Text ID	Test No.
341	U1419	A	1	H	1	W	73	0.73	0.727	6.76	13	X	1	7/11/2013 6:38	AVS	SHLF4781171	4.8E+07
341	U1419	A	1	H	3	W	65	3.65	3.635	7.692	14	X	1	7/11/2013 6:38	AVS	SHLF4781231	4.8E+07
341	U1419	A	1	H	5	W	83	6.83	6.803	10.489	19	X	1	7/11/2013 6:38	AVS	SHLF4781291	4.8E+07
341	U1419	A	2	H	2	W	37	9.27	9.213	8.391	14	X	1	7/11/2013 6:38	AVS	SHLF4781701	4.8E+07
341	U1419	A	2	H	4	W	60	12.5	12.344	10.256	12	X	1	7/11/2013 3:57	AVS	SHLF4781761	4.8E+07
341	U1419	A	2	H	6	W	60	15.5	15.252	7.459	12	X	1	7/11/2013 3:58	AVS	SHLF4781821	4.8E+07
341	U1419	A	3	H	2	W	56	18.96	18.907	13.752	19	X	1	7/11/2013 6:39	AVS	SHLF4782221	4.8E+07
341	U1419	A	3	H	4	W	27	21.67	21.548	16.083	14	X	1	7/11/2013 6:39	AVS	SHLF4782281	4.8E+07
341	U1419	A	3	H	6	W	30	24.7	24.5	12.587	14	X	1	7/11/2013 6:39	AVS	SHLF4782341	4.8E+07
341	U1419	A	6	H	1	W	55	39.45	39.45	9.79	31	X	1	7/12/2013 0:06	AVS	SHLF4783441	4.8E+07
341	U1419	A	6	H	3	W	72	42.62	42.62	11.421	26	X	1	7/12/2013 0:06	AVS	SHLF4783501	4.8E+07
341	U1419	A	6	H	5	W	45	45.35	45.35	18.414	24	X	1	7/12/2013 0:06	AVS	SHLF4783561	4.8E+07
341	U1419	A	8	H	1	W	73	58.63	58.572	31.001	19	X	1	7/11/2013 2:41	AVS	SHLF4783961	4.8E+07
341	U1419	A	8	H	3	W	67	61.66	61.364	28.437	26	X	1	7/11/2013 2:41	AVS	SHLF4784021	4.8E+07
341	U1419	A	8	H	5	W	104	65.15	64.58	25.174	26	X	1	7/11/2013 6:38	AVS	SHLF4784081	4.8E+07
341	U1419	A	9	H	1	W	48	67.88	67.876	19.58	24	X	1	7/11/2013 6:38	AVS	SHLF4784581	4.8E+07
341	U1419	A	9	H	3	W	106	71.47	71.433	40.791	19	X	1	7/11/2013 6:39	AVS	SHLF4784641	4.8E+07
341	U1419	A	9	H	5	W	57	74.01	73.95	27.505	35	X	1	7/11/2013 6:39	AVS	SHLF4784701	4.8E+07
341	U1419	A	10	H	2	W	36	76.48	76.48	25.873	33	X	1	7/11/2013 3:57	AVS	SHLF4785341	4.8E+07
341	U1419	A	10	H	4	W	72	79.82	79.82	41.024	19	X	1	7/11/2013 6:39	AVS	SHLF4785401	4.8E+07
341	U1419	A	10	H	6	W	45	82.4	82.4	30.302	24	X	1	7/11/2013 6:39	AVS	SHLF4785461	4.8E+07
341	U1419	A	11	H	2	W	26	86.06	86.023	19.58	15	X	1	7/11/2013 6:39	AVS	SHLF4785761	4.8E+07
341	U1419	A	11	H	3	W	51	87.63	87.556	30.535	26	X	1	7/11/2013 6:39	AVS	SHLF4785791	4.8E+07
341	U1419	A	12	H	2	W	56	90.16	90.147	33.798	35	X	1	7/11/2013 12:28	AVS	SHLF4786551	4.8E+07
341	U1419	A	12	H	4	W	71	93.21	93.178	25.407	27	X	1	7/11/2013 12:28	AVS	SHLF4786611	4.8E+07

Table 4: Data from Site U1421

Exp	Site	Hole	Core	Type	Sect	A/W	Offset (cm)	Depth CSF-A (m)	Depth CSF-B (m)	Vane shear strength (N/m²)	Max torque angle (deg)	Penetration direction	Vane rotation rate (deg/s)	Timestamp (UTC)	Instrument	Text ID	Test No.
341	U1421	A	1	H	1	W	71	0.71	0.708	5.594	9	X	1	7/23/2013 23:00	AVS	SHLF4834331	4.8E+07
341	U1421	A	2	H	2	W	72	9.02	8.963	7.692	14	X	1	7/23/2013 23:55	AVS	SHLF4834891	4.8E+07
341	U1421	A	2	H	4	W	87	12.17	12.032	13.985	15	X	1	7/23/2013 23:55	AVS	SHLF4834951	4.8E+07
341	U1421	A	2	H	6	W	93	15.23	15.014	16.549	21	X	1	7/23/2013 23:55	AVS	SHLF4835011	4.8E+07
341	U1421	A	3	H	2	W	64	18.44	18.404	20.978	24	X	1	7/23/2013 23:55	AVS	SHLF4835601	4.8E+07
341	U1421	A	3	H	4	W	89	21.69	21.6	11.888	17	X	1	7/23/2013 23:55	AVS	SHLF4835661	4.8E+07
341	U1421	A	3	H	6	W	55	24.35	24.216	12.587	14	X	1	7/23/2013 23:55	AVS	SHLF4835721	4.8E+07
341	U1421	A	4	H	1	W	97	26.77	26.77	14.452	49	X	1	7/23/2013 23:55	AVS	SHLF4836281	4.8E+07
341	U1421	A	6	H	2	W	72	47.02	46.994	69.927	28	X	1	7/23/2013 23:55	AVS	SHLF4836581	4.8E+07
341	U1421	A	6	H	4	W	60	49.9	49.841	35.197	19	X	1	7/23/2013 23:55	AVS	SHLF4836641	4.8E+07
341	U1421	A	7	H	2	W	95	53.25	53.197	32.166	31	X	1	7/23/2013 23:55	AVS	SHLF4837111	4.8E+07
341	U1421	A	7	H	4	W	75	56.05	55.937	28.437	21	X	1	7/23/2013 23:55	AVS	SHLF4837171	4.8E+07
341	U1421	A	7	H	6	W	81	59.01	58.833	32.166	31	X	1	7/23/2013 23:55	AVS	SHLF4837231	4.8E+07
341	U1421	A	8	H	1	W	26	60.56	60.558	78.784	49	X	1	7/23/2013 23:55	AVS	SHLF4837531	4.8E+07
341	U1421	A	8	H	2	W	39	62.19	62.176	79.251	28	X	1	7/23/2013 23:55	AVS	SHLF4837561	4.8E+07
341	U1421	A	8	H	4	W	42	65.22	65.183	69.927	37	X	1	7/23/2013 23:55	AVS	SHLF4837621	4.8E+07
341	U1421	A	9	H	2	W	36	67.36	67.322	42.189	40	X	1	7/23/2013 23:55	AVS	SHLF4837961	4.8E+07
341	U1421	A	9	H	3	W	25	68.75	68.683	49.182	47	X	1	7/23/2013 23:56	AVS	SHLF4837991	4.8E+07
341	U1421	A	10	H	1	W	24	70.44	70.415	23.542	42	X	1	7/23/2013 23:54	AVS	SHLF4838481	4.8E+07
341	U1421	A	11	H	2	W	37	72.67	72.579	52.911	50	X	1	7/23/2013 23:54	AVS	SHLF4838771	4.8E+07
341	U1421	A	11	H	4	W	35	75.16	74.948	45.219	26	X	1	7/23/2013 23:54	AVS	SHLF4838831	4.8E+07
341	U1421	A	12	H	1	W	67	76.17	76.139	61.303	37	X	1	7/23/2013 23:54	AVS	SHLF4839131	4.8E+07
341	U1421	A	12	H	3	W	93	79.43	79.247	32.166	26	X	1	7/23/2013 23:54	AVS	SHLF4839191	4.8E+07
341	U1421	A	13	H	1	W	74	80.94	80.926	76.454	35	X	1	7/23/2013 23:54	AVS	SHLF4839311	4.8E+07
341	U1421	A	13	H	2	W	76	82.46	82.417	59.205	38	X	1	7/23/2013 23:55	AVS	SHLF4839341	4.8E+07
341	U1421	A	14	H	1	W	75	84.05	84.033	48.25	30	X	1	7/23/2013 23:55	AVS	SHLF4839721	4.8E+07
341	U1421	A	17	H	1	W	80	89.2	89.2	61.07	33	X	1	7/23/2013 23:55	AVS	SHLF4840481	4.8E+07
341	U1421	A	17	H	2	W	59	90.49	90.49	48.017	32	X	1	7/23/2013 23:55	AVS	SHLF4840511	4.8E+07
341	U1421	A	19	H	1	W	74	93.94	93.94	47.783	40	X	1	7/23/2013 23:55	AVS	SHLF4840951	4.8E+07
341	U1421	A	19	H	2	W	43	95.13	95.13	57.107	31	X	1	7/23/2013 23:55	AVS	SHLF4840981	4.8E+07